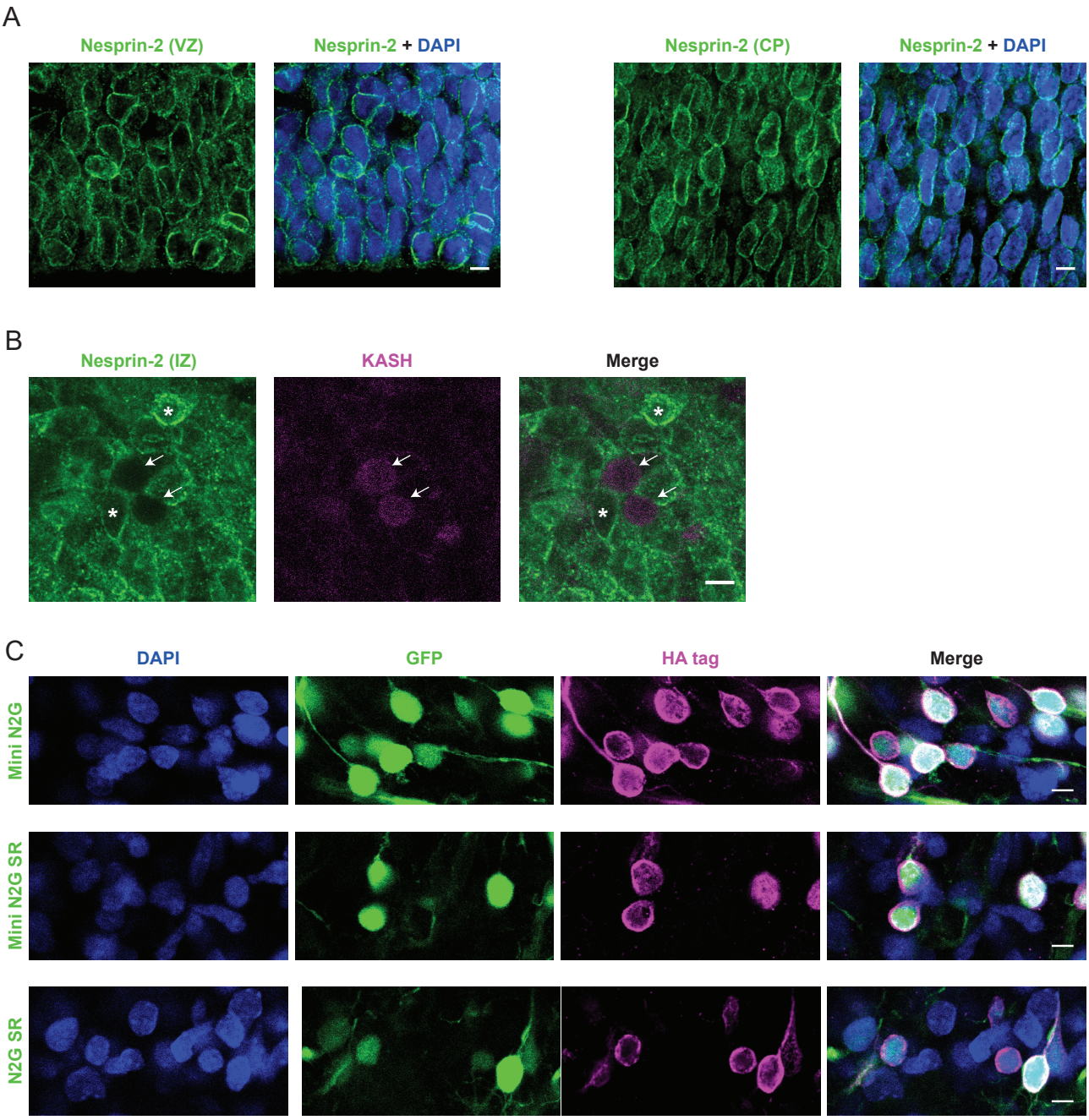
A
Nesprin-2 (VZ)
Nesprin-2 + DAPI
Nesprin-2 (CP)
Nesprin-2 + DAPI
B
Nesprin-2 (IZ)
KASH
Merge
C
DAPI
GFP
HA tag
Merge
Mini N2G
Mini N2G SR
N2G SR

Figure S1. Distribution of endogenous Nesprin-2 and expressed Nesprin-2 functional domains in embryonic rat brain. Related to Figure 1. (A) Embryonic day 20 (E20) rat brain slices were stained with DAPI and for Nesprin-2, and representative images from the Ventricular Zone (VZ) and Cortical Plate (CP) are shown. Nesprin-2 decorates the Nuclear Envelope (NE) of cells in the VZ and the CP. **(B)** E16 rat brain was electroporated with a KASH-RFP fragment (in magenta), and subsequently imaged fixed at E20. Electroporated brains were stained for endogenous Nesprin-2 and images from the Intermediate Zone (IZ) are depicted. While endogenous Nesprin-2 decorates the nucleus of non-electroporated cells (asterisks), neurons expressing the KASH dominant negative fragment do not exhibit Nesprin-2 at the NE (arrows), consistent to that reported in other systems [S1,S2]. **(C)** E16 rat brain was electroporated with the Nesprin-2 constructs, and subsequently imaged at E20. Electroporated brains were stained with DAPI and the HA epitope tag, and fixed images from the IZ are shown. Expressed constructs were successfully targeted to the NE. **A**, **B** and **C** scale bars, 5µm.

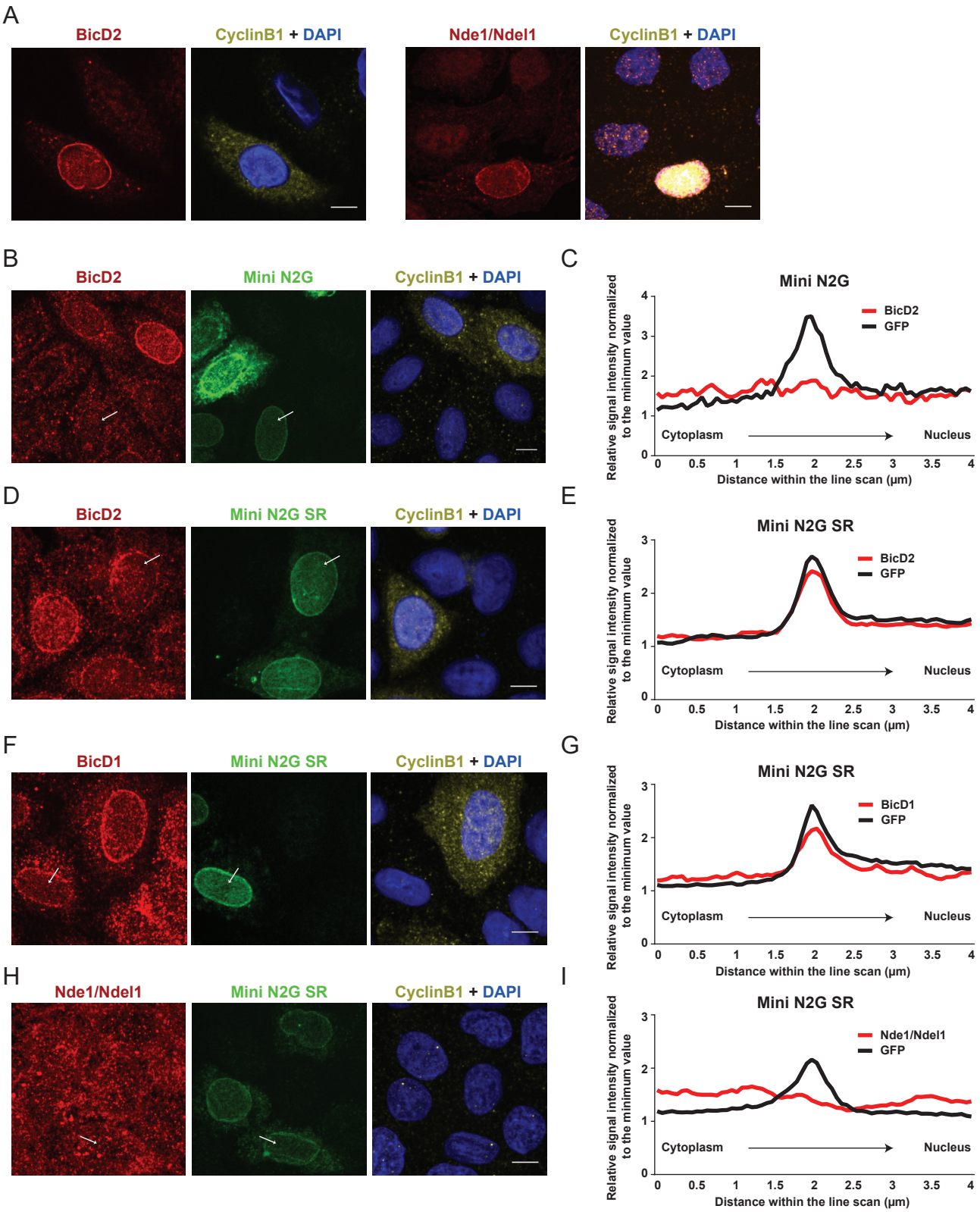
A
BicD2
CyclinB1 + DAPI
Nde1/Ndel1
CyclinB1 + DAPI
B
BicD2
Mini N2G
CyclinB1 + DAPI
C
Mini N2G
BicD2
GFP
Relative signal intensity normalized to the minimum value
Cytoplasm
Nucleus
Distance within the line scan (μm)
D
BicD2
Mini N2G SR
CyclinB1 + DAPI
E
Mini N2G SR
BicD2
GFP
Relative signal intensity normalized to the minimum value
Cytoplasm
Nucleus
Distance within the line scan (μm)
F
BicD1
Mini N2G SR
CyclinB1 + DAPI
G
Mini N2G SR
BicD1
GFP
Relative signal intensity normalized to the minimum value
Cytoplasm
Nucleus
Distance within the line scan (μm)
H
Nde1/Ndel1
Mini N2G SR
CyclinB1 + DAPI
I
Mini N2G SR
Nde1/Ndel1
GFP
Relative signal intensity normalized to the minimum value
Cytoplasm
Nucleus
Distance within the line scan (μm)

Figure S2. Test for BicD1, BicD2 and Nde1/Ndel1 co-localization with Nesprin-2 in cultured non-neuronal cells. Related to Figure 3. (A) Representative images of cultured HeLa cells fixed and stained with DAPI and for endogenous BicD2, Nde1/Ndel1, and Cyclin B1. In Cyclin B-positive G2 cells, BicD2 and Nde1/Ndel1 each accumulated at the NE, consistent with published data [S1,S3–5]. **(B-E)** Cultured HeLa cells transfected with GFP-tagged Mini N2G and Mini N2G SR were stained with DAPI and for endogenous BicD2 and Cyclin B1. Intensity scans were performed along lines depicted by arrows of 4µm length starting in the cytoplasm and ending within the nucleus. **(B, D)** Representative fixed images and **(C, E)** line scan quantifications are shown. BicD2 was enhanced at the NE in non-G2 cells that expressed Mini N2G SR, though not in Mini N2G-expressing cells. **(F-I)** Cultured HeLa cells transfected with GFP-tagged Mini N2G SR were stained with DAPI and for endogenous BicD1, Nde1/Ndel1 and Cyclin B1. Scans were performed along lines depicted by arrows. **(F, H)** Representative fixed images and **(G, I)** line scan quantifications are shown. BicD1, but not Nde1/Ndel1 accumulated at the NE in non-G2 cells that expressed Mini N2G SR. Data presented as superimposed symbols at mean with a connecting line in **C, E, G** and **I**. Data in **C, E, G** and **I** include line scan analysis from at least 7 cells. **A, B, D, F** and **H** scale bar, 10µm.

A

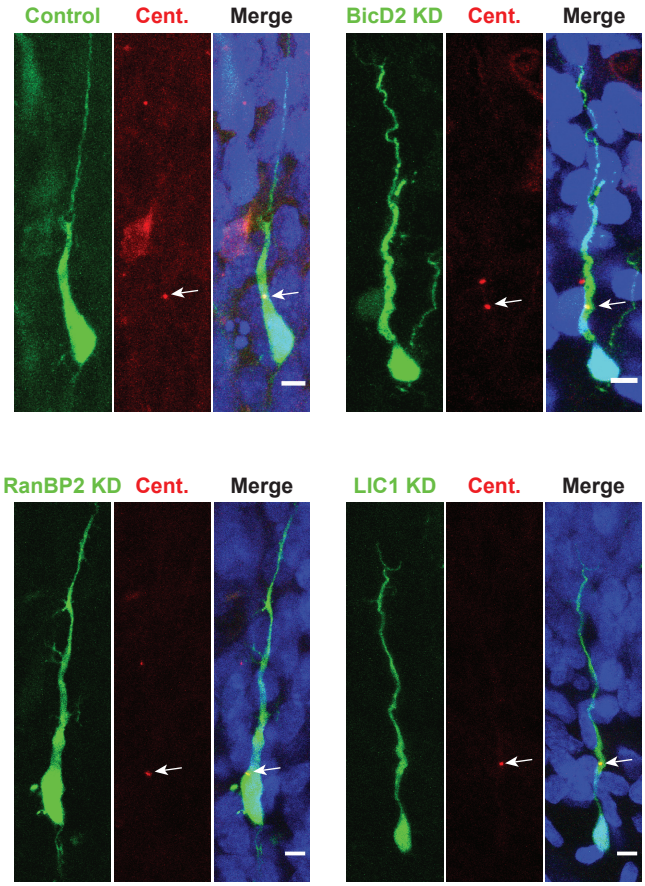
Control
Cent.
Merge
BicD2 KD
Cent.
Merge
RanBP2 KD
Cent.
Merge
LIC1 KD
Cent.
Merge

B

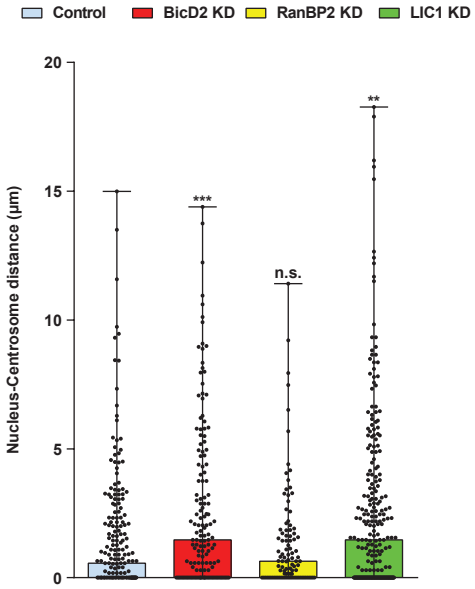
Control
BicD2 KD
RanBP2 KD
LIC1 KD
Nucleus-Centrosome distance (μm)
20
15
10
5
0
***
n.s.
**

Figure S3. Effects of BicD2, RanBP2 or LIC1 shRNAs in Nucleus-Centrosome coupling. Related to Figure 4. (A-B) E16 rat brain was electroporated with control vector, BicD2, RanBP2, or Light Intermediate Chain 1 (LIC1) shRNAs together with PACT-DsRed, and subsequently imaged in fixed brain sections prepared at E20. **(A)** Representative images of electroporated neurons in the CP showing centrosome (Cent) position (arrow) relative to that of the soma. **(B)** Quantification of N-C distance reveals an increase for BicD2 and LIC1, but not RanPB2 RNAi. BicD2 interacts with dynein mainly via the dynein LIC1 subunit [S6], and consistent with a role for BicD2/LIC1 dynein in post-mitotic nuclear migration, BicD2 RNAi caused an equivalent increase in N-C separation to that of dynein LIC1. Data presented as scatter dot plot with bar representing median with range in **B**. Mann Whitney test for non-parametric distributions was used in **B** (**P<0.01; ***P<0.001; n.s. non-significant). Data in **B** include at least 100 electroporated neurons from at least 2 embryos, per condition. **A** scale bar, 5µm.

A

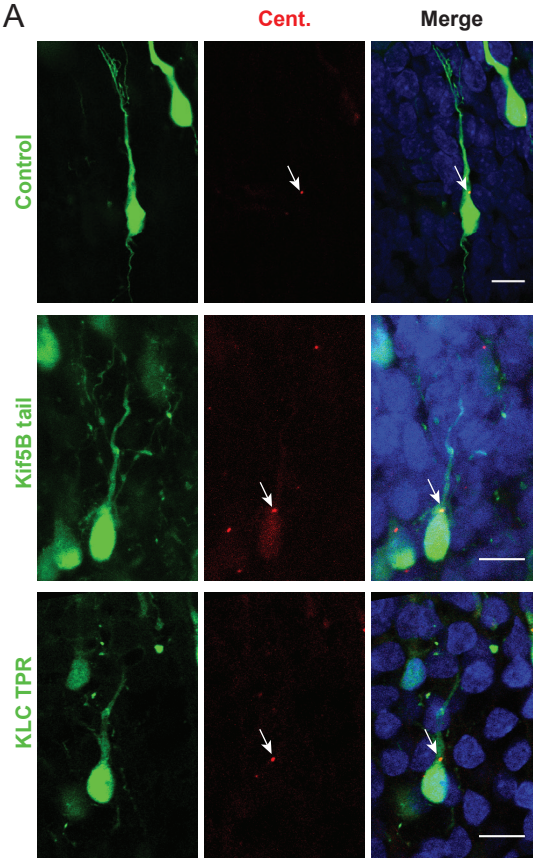
Cent.
Merge
Control
Kif5B tail
KLC TPR

B

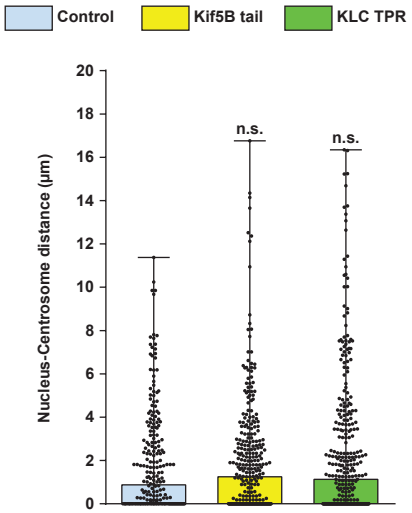
Control
Kif5B tail
KLC TPR
Nucleus-Centrosome distance (μm)
0
2
4
6
8
10
12
14
16
18
20
n.s.
n.s.

Figure S4. Effect of Kif5B tail and KLC TPR domains on nucleus-centrosome coupling. Related to Figure 5. (A, B) E16 rat brain was electroporated with control, Kif5B tail or KLC TPR cDNAs together with PACT-DsRed, and imaged in fixed brain sections at E20. **(A)** Representative images of electroporated neurons in the CP showing centrosome (Cent.) position (arrow) relative to that of the soma. **(B)** Quantification of N-C distance revealed no significant effect of kinesin-1 inhibition on N-C spacing. Data presented as scatter dot plot with bar representing median with range in **B**. Mann Whitney test for non-parametric distributions was used in **B** (n.s. non-significant). Data in **B** include at least 317 electroporated cells from at least 3 embryos, per condition. **B** scale bar, 10µm.

Supplemental References

S1. Hu, D.J.-K., Baffet, A.D.D., Nayak, T., Akhmanova, A., Vallee, R.B.B., Doye, V., and Vallee, R.B.B. (2013). Dynein Recruitment to Nuclear Pores Activates Apical Nuclear Migration and Mitotic Entry in Brain Progenitor Cells. Cell *154*, 1300–1313.

S2. Luxton, G.W.G., Gomes, E.R., Folker, E.S., Vintinner, E., and Gundersen, G.G. (2010). Linear arrays of nuclear envelope proteins harness retrograde actin flow for nuclear movement. Science *329*, 956–9.

S3. Splinter, D., Tanenbaum, M.E., Lindqvist, A., Jaarsma, D., Flotho, A., Yu, K. Lou, Grigoriev, I., Engelsma, D., Haasdijk, E.D., Keijzer, N., *et al.* (2010). Bicaudal D2, dynein, and kinesin-1 associate with nuclear pore complexes and regulate centrosome and nuclear positioning during mitotic entry. PLoS Biol. *8*.

S4. Baffet, A.D., Hu, D.J., and Vallee, R.B. (2015). Cdk1 Activates Pre-mitotic Nuclear Envelope Dynein Recruitment and Apical Nuclear Migration in Neural Stem Cells. Dev. Cell *33*, 703–716.

S5. Bolhy, S., Bouhlel, I., Dultz, E., Nayak, T., Zuccolo, M., Gatti, X., Vallee, R., Ellenberg, J., and Doye, V. (2011). A Nup133-dependent NPC-anchored network tethers centrosomes to the nuclear envelope in prophase. J. Cell Biol. *192*, 855–871.

S6. Gonçalves, J.C., Dantas, T.J., and Vallee, R.B. (2019). Distinct roles for dynein light intermediate chains in neurogenesis, migration, and terminal somal translocation. J. Cell Biol. *218*, 808–819.